Thin Oxide Films

DOI: 10.1002/anie.201107097

The Atomic Structure of a Metal-Supported Vitreous Thin Silica Film**

Leonid Lichtenstein, Christin Büchner, Bing Yang, Shamil Shaikhutdinov, Markus Heyde, Marek Sierka, Radosław Włodarczyk, Joachim Sauer, and Hans-Joachim Freund*

Silica glass has been extensively studied.[1–6] Yet, we know little about its atomic-scale structure. In 1932, Zachariasen postulated that vitreous silica consists of a continuous random network of corner-sharing SiO_4 tetrahedra.[8,9] He assumed that the nature of the bonding forces between the atoms of a glass is essentially the same as in a crystal. This assumption has never been verified microscopically with true atomic resolution. As it is difficult to apply scanning-probe techniques to a three dimensional (3D) amorphous material, a two dimensional (2D) equivalent system would have to be prepared to make the observation possible.

Thin oxide films on metal substrates have proven to be very useful model systems.[10,11] Furthermore, thin oxide films may be investigated using standard surface-science tools. Thin crystalline silica films were grown on Mo(112)[12,13] consisting of a highly ordered honeycomb-like single layer of corner sharing SiO_4 tetrahedra,[14] however with $SiO_{2.5}$ composition. Growing the film thicker resulted in a rough and amorphous surface, which is most probably due to strong Si-O-Mo bonds at the interface already present in the monolayer.[15]

To obtain a better model system for silica, a film with the correct SiO_2 composition has to be prepared. We recently reported on a crystalline silica bilayer sheet grown on Ru(0001).[16] This system meets the required composition, because it consists of a cage-like structure made of corner-sharing SiO_4 tetrahedra building a fully saturated structure, which is weakly bound to the metal.

Herein, we address the atomic structure of a vitreous thin silica bilayer film grown on Ru(0001). We applied low-temperature scanning tunneling microscopy (STM) in ultra high vacuum (UHV). For the first time, the atomic structure of a silica glass was resolved in real space. Studying the local atomic structure of an amorphous or vitreous thin silica film provides the possibility to investigate fundamental aspects of glasses.

In contrast to our previous publication on the ordered bilayer silica on Ru(0001),[16] we used slightly different preparation conditions (see Experimental Section).

The preparation presented herein results in the Ru substrate being almost completely covered (95%) by a flat and amorphous bilayer of silica. Figure 1 shows the complex atomic arrangement of the thin film. High resolution STM revealed a 2D network of polygons (see Figure 1 a).

The imaged polygonal network exhibits a small internal corrugation of approximately 20 pm. We observed that all the protrusions were arranged in triangles. Based on this triangular symmetry we assigned the protrusions to one side of a tetrahedral SiO_4 building block. Consequently, the protrusions are triangles of three O atoms (red dots in Figure 1). Sensitivity of STM to the Si positions would result in a different local structure. To find the position of the Si atoms, we calculated the circumscribed circle around every O

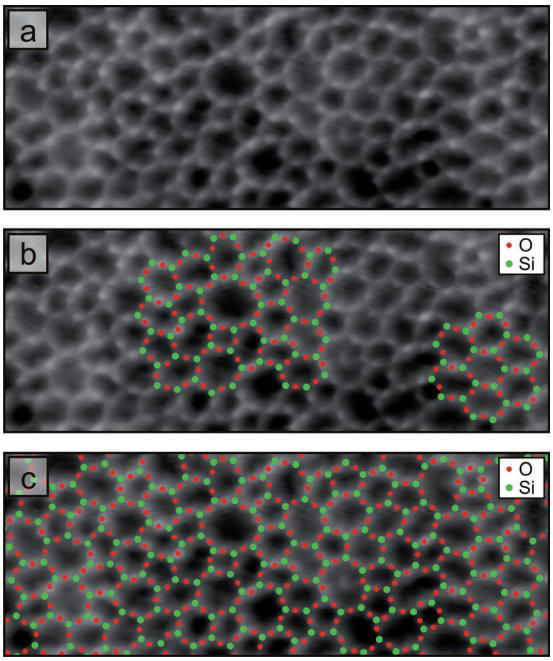

Figure 1. Atomic resolution STM image of a vitreous silica film on Ru(0001). a) Constant current STM image. Scan range 8.0×3.0 nm^2, $V_S = 100$ mV, $I_T = 100$ pA. b) Same image as in (a), partly superimposed with a model. Bright protrusions are identified as O atoms (red dots). Si positions (green dots) were calculated from circles circumscribed around every O triangle. Ordered (right side) and amorphous (left side) areas are visible. c) Complete model. All atoms are arranged in SiO_3 triangles corresponding to SiO_4 tetrahedra in 3D.

[*] L. Lichtenstein, C. Büchner, Dr. B. Yang, Dr. S. Shaikhutdinov, Dr. M. Heyde, Prof. H.-J. Freund
Department of Chemical Physics
Fritz-Haber-Institut der Max-Planck-Gesellschaft
Faradayweg 4–6, 14195 Berlin (Germany)
E-mail: heyde@fhi-berlin.mpg.de
Homepage: http://www.fhi-berlin.mpg.de/cp/
Dr. M. Sierka, R. Włodarczyk, Prof. J. Sauer
Institut für Chemie, Humboldt-Universität zu Berlin
Brook-Taylor-Strasse 2, 12489 Berlin (Germany)

[**] We thank the German Science Foundation (DFG) as well as the Fonds der Chemischen Industrie for financial support. We also thank Piero Ugliengo (Turin) for communicating unpublished energies from Refs. [7,8].

Supporting information for this article is available on the WWW under http://dx.doi.org/10.1002/anie.201107097.

triangle. By placing a green dot (Figure 1) corresponding to a Si atom in the center of each resulting circle, we completed the 2D model of the topmost O and Si atoms. Figure 1b illustrates two areas covered with such a model. On the right side we identify a crystalline area consisting of several silica hexagons showing the same orientation and dimension as in Ref. [16]. However, on the left side, the film showed rings of different size and did not exhibit any crystalline order.

The amorphous structure of the thin silica film is consistent with a weak coupling to the metal support. The orientation of the crystalline areas coincided with the lattice directions of the Ru support. However, at the amorphous regions, the registry to the substrate was lost. Thus, the film is structurally decoupled from the metal support.

In Figure 1c the STM image is completely covered by the structural model. All the O atoms were arranged in triangles. In 3D, this structure corresponds to a network of corner-sharing SiO_4 tetrahedra. While the film is amorphous in the *xy*-plane (substrate plane), it is highly ordered in the *z*-direction. The SiO_4 tetrahedra of the first layer are linked by bridging O atoms to the SiO_4 units of the second layer with a Si-O-Si angle of 180°. The linking O atoms represent a mirror plane. This particular structural element leads to a flat and 2D film. The film structure consists of four-membered rings standing upright and connected randomly, forming the 2D ring network.

The density of the vitreous silica film was calculated from the bilayer model adapted from Figure 1c. The total 2D density was 16.8 $SiO_2\,nm^{-2}$. Hence, the vitreous silica film is more densely packed than the crystalline which had a 2D density of 15.9 $SiO_2\,nm^{-2}$.[16]

Note that we only use the topmost O and Si positions derived from the STM image for the following statistical evaluation presented in Figure 2 and Figure 3. To compensate for the lack of information in the third dimension, we took the height difference between the topmost Si and O from the density functional theory (DFT) model for the crystalline silica bilayer (52 pm).[16]

A statistical analysis of the ring size and two characteristic angles is presented in Figure 2. Figure 2a visualizes the silica polygons of different size. Note that only Si atoms are shown in this scheme (as green balls). Strikingly, the environment of a ring depends on its size. Rings with more than six Si atoms tend to be surrounded by smaller rings. The ring arrangement is governed by the possible angles inside an SiO_4 tetrahedron and angles connecting two tetrahedra.

A histogram of the ring size is depicted in Figure 2b. Note that for the histograms a slightly larger area ($10 \times 4\ nm^2$) was evaluated than shown in Figure 1. The smallest rings in the STM image consisted of four Si atoms and the biggest of nine Si atoms. The most common ring had six Si atoms. The distribution was asymmetric around the maximum.

In addition, we computed all O-Si-O angles in the model (see histogram in Figure 2c). The intra-tetrahedral angle showed a symmetric distribution with an average of 110° and a standard deviation of 10°. This value corresponds well with the 109.5° angle in a regular tetrahedron.

The histogram of the Si-O-Si angles is shown in Figure 2d. We observed a peak at 141°. This angle is in agreement to the

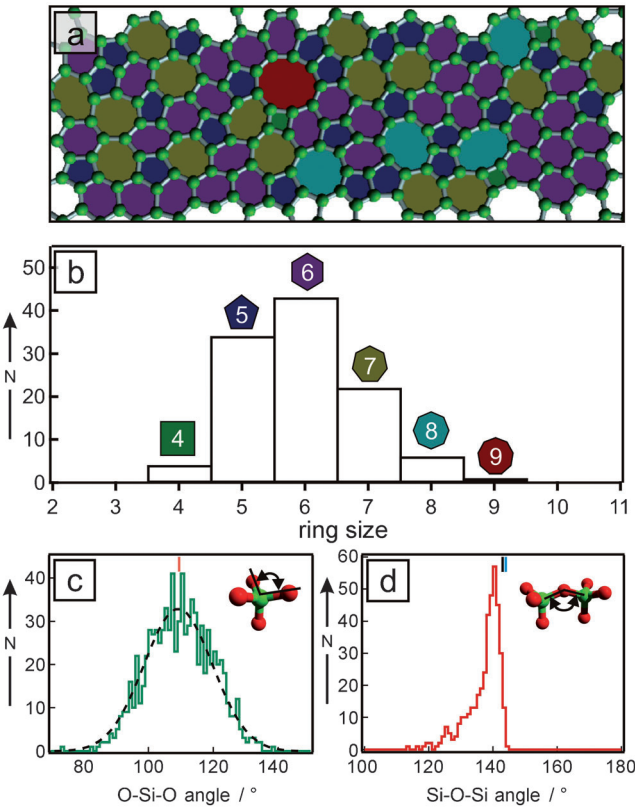

Figure 2. Structure statistics. a) Model adapted from the STM image in Figure 1a. Only Si atoms are shown (green balls). Rings with the same number of Si atoms have the same color. b) Histogram of the differently sized silica rings. c) Histogram of the O-Si-O-angle. The red bar indicates the regular tetrahedral angle of 119.5°. d) Histogram of the Si-O-Si angle. Bars indicate average values from a ^{29}Si MAS NMR study (black)[17] and an X-ray diffraction study (blue),[4] both on vitreous silica.

average angle of 143° obtained in a ^{29}Si magic-angle spinning nuclear magnetic resonance spectroscopy (^{29}Si MAS NMR)[17] and 144° in an X-ray diffraction study,[4] both on vitreous silica. Furthermore, we observed a sharp edge in the histogram of the Si-O-Si angles at 145°. This sharp boundary underlines the flat and 2D character of the silica bilayer film.

A useful way to characterize the atomic order in a material is to compute the pair correlation function (PCF). The great advantage of this method is the direct comparison to PCFs derived from diffraction experiments using a Fourier transformation. We calculated the PCF for our model and compared it to literature values (see Figure 3).

Figure 3a shows pair distance histograms for Si–O (blue), O–O (red), and Si–Si (green) from the STM model. First peaks in all three distributions correspond to the respective nearest neighbor distances. The first Si–O peak is at 156 ± 14 pm. Taking into account that we fixed the Si–O distance in every O triangle, the sharp peak means that the Si–O distance fluctuation throughout the image was small. The first O–O peak is located at 258 ± 32 pm. The large standard deviation can be explained by the experimental difficulty of defining the exact O position. The first Si–Si peak is situated at 296 ± 14 pm. The smaller standard deviation is due to the calculation procedure of the Si positions. The amorphous nature of

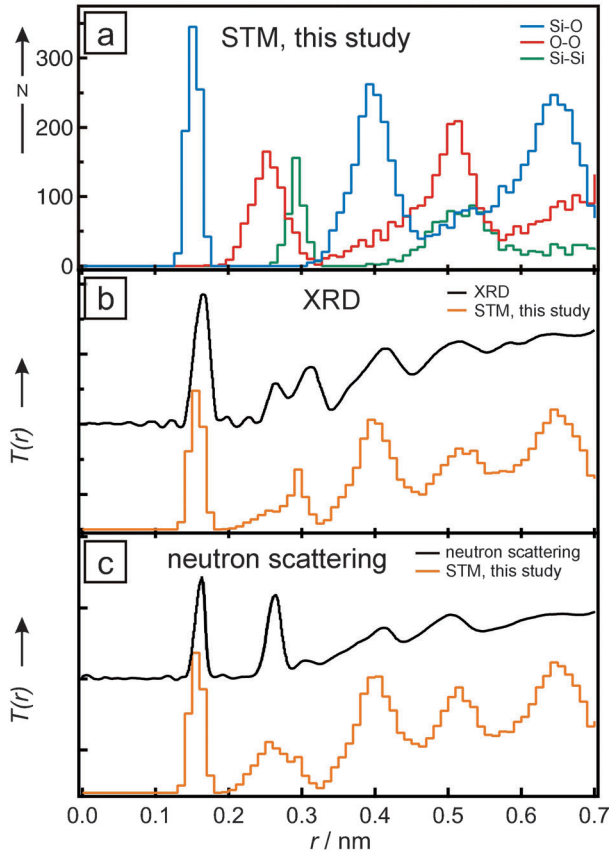

Figure 3. Pair correlation function. a) The pair distance histograms for Si–O (blue), O–O (red), and Si–Si (green). b) Comparison of the total pair correlation function, $T_{STM}(r)$ (orange curve), with the PCF obtained from X-ray diffraction measurements on vitreous silica (black curve).[4] c) Comparison of $T_{STM}(r)$ (orange curve) with results from neutron scattering on vitreous silica (black curve).[18]

the film is reflected in the peaks getting broader for larger radial distances.

We found good agreement between the PCF of the vitreous silica film and the PCFs obtained in diffraction studies of vitreous silica. The total pair correlation function of the experimentally derived structural model, $T_{STM}(r)$, was obtained using X-ray and neutron scattering factors of Si and O according to the formula in Refs. [19,20]. $T_{STM}(r)$ was additionally normalized by r^{-1} to account for the 2D structure of the thin film. Figure 3b gives a comparison between $T_{STM}(r)$ and the PCF obtained in an X-ray diffraction experiment, which was carried out up to a radial distance of 0.7 nm.[4] In Figure 3c, we compare $T_{STM}(r)$ to neutron scattering measurements.[18] The short-range and the medium-range order are reproduced. The major peak positions and their relative magnitudes of $T_{STM}(r)$ indicate reasonable agreement with the X-ray and neutron PCF. The small deviations are because the silica bilayer on Ru(0001) is flat in contrast to 3D silica glass studied in diffraction experiments.

To estimate the energy needed to form the amorphous film we performed DFT calculations for the simplest model of an ordered film with a defect, which consists of two 5- and two 7-membered rings embedded in a 5×3 surface unit cell (Figure 4a). Formally, this structure can be obtained by a rotation of one of the $(SiO_2)_4$ units (Figure 4b). Our estimate for its energy is 177 kJ mol^{-1} per unit cell above that of the ordered film. In line with experiment, the equilibrium structure of the defective film shows slightly higher surface density than the ordered one (16.6 vs. 16.4 SiO_2 nm^{-2}). We generated several additional models containing silica rings of different sizes with energies between 250 and 310 kJ mol^{-1} per unit cell above that of the ordered film (Figure 4c, side view in Figure 4e). Thus, the energy difference between different amorphous structures is smaller than the difference between the amorphous structure and the crystalline one. Since at least 32 SiO_2 units are involved in the transition shown in Figure 4b, per SiO_2 unit the amorphous structures shown in Figure 4a and c are 5.5–9.6 kJ mol^{-1} higher in energy than the ordered film. For bulk silica, even larger differences have been obtained. Per SiO_2 unit, a model of vitreous silica[7] is 21.1 kJ mol^{-1} higher in energy than α-quartz.[8,21] These results suggest that the amorphous structure is a metastable phase. Indeed, the estimated barrier for its transition into the

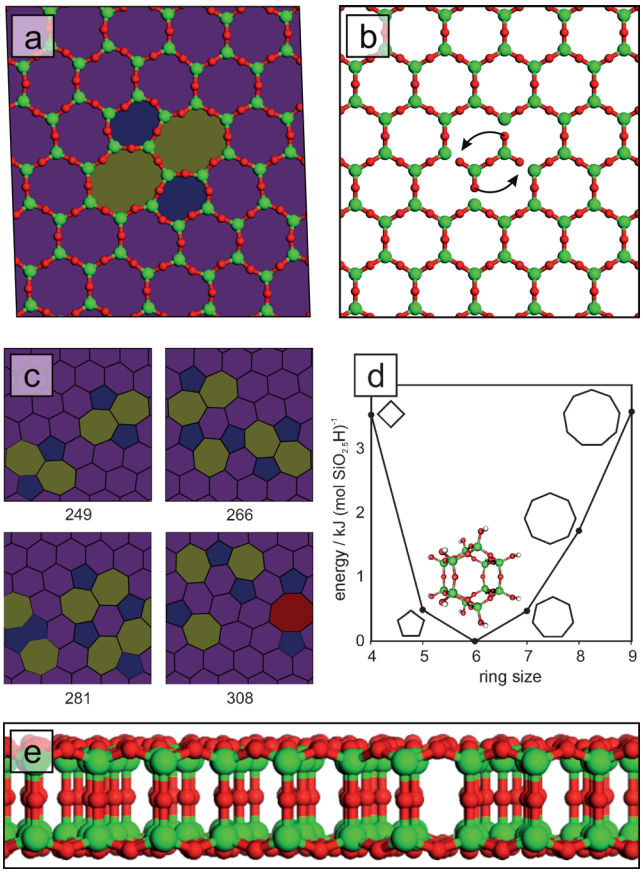

Figure 4. a) The simplest model of an amorphous film consisting of two 5- and two 7-membered rings embedded in a 5×3 surface unit cell of the ordered film. b) The rotation of one of the $(SiO_2)_4$ units which leads to the model shown in (a). c) Different models of an amorphous film and their relative energies (kJ mol^{-1}) with respect to the ordered film. A side view of the bottom left model is given in (e). d) Relative energies of the isolated hydroxylated double silica rings with composition $(SiO_{2.5}H)_{2n}$, where n is the Si-O-Si ring size. The atomic structure of the 6-membered ring is shown. (Si green, O red, H gray).

ordered film (the process shown in Figure 4b) is high, 338 kJ mol^{-1} per Si–O bond involved (2704 kJ mol^{-1} for all 8 Si–O bonds). Formation of such metastable phases is kinetically controlled. In the present case, the process may start from isolated silica rings and double rings, whose energy is known to vary little for ring sizes between four and eight.[22,23] The present DFT calculations confirm that isolated silica double rings, models of crystallization centers of the amorphous film, are quite close in energy (Figure 4d).

In summary, we prepared an atomically flat and extended vitreous thin silica film on Ru(0001). STM revealed the thin film's atomic arrangement consisting of corner-sharing SiO_4 units. These silica building blocks formed a complex network which lacked long-range order and registry to the substrate. The decoupling could play a crucial role in investigating single atoms incorporated into the cage structure. By building a model of the topmost Si and O atoms based on the STM image, we made a statistical analysis of the structure. Histograms of ring sizes and angles were given. A comparison between the PCF derived from our experimental model and the PCF obtained in diffraction experiments on vitreous silica was drawn and showed satisfying agreement. DFT calculations also suggest that the amorphous film is a metastable phase. The vitreous silica model system, which can be investigated by well-established surface science tools, provides the unique possibility to study glass and the glass transition with atomic resolution in real space.

Experimental Section

To study the atomic structure, we simultaneously applied STM and frequency modulated dynamic force microscopy (FM-DFM) (also known as noncontact atomic force microscopy, NC-AFM) using a tuning-fork sensor with a PtIr tip. All experiments were performed at low temperature (5 K) in UHV. The vitreous silica bilayer film was prepared using a method similar to that described in Ref. [16]. Prior to film preparation, we cleaned the Ru(0001) sample by cycles of Ar^+ bombardment and annealing to 1300 °C. The cleanliness of the metal surface was controlled using low-energy electron diffraction, Auger electron spectroscopy, and STM. For the preparation of the silica film, we deposited Si on a (2×2)-3O precovered Ru(0001)-sample in an O_2 atmosphere of 2×10^{-7} mbar. Afterwards, the sample was annealed to 950 °C in 5×10^{-6} mbar O_2 for 10 min. The cooling rate after annealing was one of the critical parameters for the formation of an amorphous structure. In general, amorphous materials are formed by fast cooling after high-temperature annealing.[24] In this manner, the crystallization process is bypassed.

Periodic DFT calculations have been performed using the Vienna Ab initio Simulation Package (VASP)[25] along with the Perdew, Burke, and Ernzerhof (PBE)[26] exchange-correlation functional. The electron–ion interactions were described by the projector augmented wave method (PAW), originally developed by Blöchl[27] and adapted by Kresse and Joubert.[28] DFT calculations of molecular models were performed using the TURBOMOLE program package[29–31] employing the B3-LYP hybrid exchange-correlation functional[32,33] and triple zeta valence plus polarization (TZVP) basis sets.[34] To speedup DFT calculations we use the multipole accelerated resolution of identity (MARI-J) method[35] along with the TZVP auxiliary basis sets.[36,37]

Received: October 6, 2011
Published online: November 24, 2011

Keywords: amorphous structures · glass · scanning probe techniques · silica · thin films

[1] B. E. Warren, J. Biscce, *J. Am. Ceram. Soc.* **1938**, *21*, 49.
[2] D. L. Evans, S. V. King, *Nature* **1966**, *212*, 1353.
[3] R. J. Bell, P. Dean, *Nature* **1966**, *212*, 1354.
[4] R. L. Mozzi, B. E. Warren, *J. Appl. Crystallogr.* **1969**, *2*, 164.
[5] A. C. Wright, *J. Non-Cryst. Solids* **1994**, *179*, 84.
[6] W. Raberg, A. H. Ostadrahimi, T. Kayser, K. Wandelt, *J. Non-Cryst. Solids* **2005**, *351*, 1089.
[7] M. Corno, A. Pedone, R. Dovesi, P. Ugliengo, *Chem. Mater.* **2008**, *20*, 5610.
[8] F. Musso, M. Sodupe, M. Corno, P. Ugliengo, *J. Phys. Chem. C* **2009**, *113*, 17876.
[9] W. H. Zachariasen, *J. Am. Chem. Soc.* **1932**, *54*, 3841.
[10] H.-J. Freund, *Catal. Today* **2005**, *100*, 3.
[11] H.-J. Freund, G. Pacchioni, *Chem. Soc. Rev.* **2008**, *37*, 2224.
[12] X. Xu, D. W. Goodman, *Appl. Phys. Lett.* **1992**, *61*, 774.
[13] T. Schroeder, M. Adelt, B. Richter, M. Naschitzki, M. Bäumer, H.-J. Freund, *Surf. Rev. Lett.* **2000**, *7*, 7.
[14] J. Weissenrieder, S. Kaya, J.-L. Lu, H.-J. Gao, S. Shaikhutdinov, H.-J. Freund, M. Sierka, T. K. Todorova, J. Sauer, *Phys. Rev. Lett.* **2005**, *95*, 076103.
[15] D. J. Stacchiola, M. Baron, S. Kaya, J. Weissenrieder, S. Shaikhutdinov, H.-J. Freund, *Appl. Phys. Lett.* **2008**, *92*, 011911.
[16] D. Löffler, J. J. Uhlrich, M. Baron, B. Yang, X. Yu, L. Lichtenstein, L. Heinke, C. Büchner, M. Heyde, S. Shaikhutdinov, H.-J. Freund, R. Wlodarczyk, M. Sierka, J. Sauer, *Phys. Rev. Lett.* **2010**, *105*, 146104.
[17] L. F. Gladden, T. A. Carpenter, S. R. Elliott, *Philos. Mag. B* **1986**, *53*, 81.
[18] D. I. Grimley, A. C. Wright, R. N. Sinclair, *J. Non-Cryst. Solids* **1990**, *119*, 49.
[19] R. J. Bell, P. Dean, *Philos. Mag.* **1972**, *25*, 1381.
[20] L. F. Gladden, *J. Non-Cryst. Solids* **1990**, *119*, 318.
[21] P. Ugliengo, personal communication.
[22] J.-R. Hill, J. Sauer, *J. Phys. Chem.* **1994**, *98*, 1238.
[23] V. Moravetski, J.-R. Hill, U. Eichler, A. K. Cheetham, J. Sauer, *J. Am. Chem. Soc.* **1996**, *118*, 13015.
[24] R. Zallen in *The Physics of Amorphous Solids*, Wiley, New York, **1983**, p. 5.
[25] a) G. Kresse, J. Furthmüller, *Comput. Mater. Sci.* **1996**, *6*, 15; b) G. Kresse, J. Furthmüller, *Phys. Rev. B* **1996**, *54*, 11169.
[26] J. P. Perdew, K. Burke, M. Ernzerhof, *Phys. Rev. Lett.* **1996**, *77*, 3865; J. P. Perdew, K. Burke, M. Ernzerhof, *Phys. Rev. Lett.* **1997**, *78*, 1396.
[27] P. E. Blöchl, *Phys. Rev. B* **1994**, *50*, 17953.
[28] G. Kresse, D. Joubert, *Phys. Rev. B* **1999**, *59*, 1758.
[29] TURBOMOLE V5.9 2008, a development of University of Karlsruhe and Forschungszentrum Karlsruhe GmbH, **1989–2007**, TURBOMOLE GmbH, since 2007; available from http://www.turbomole.com.
[30] R. Ahlrichs, M. Bär, M. Häser, H. Horn, C. Kölmel, *Chem. Phys. Lett.* **1989**, *162*, 165.
[31] O. Treutler, R. Ahlrichs, *J. Chem. Phys.* **1995**, *102*, 346.
[32] A. D. Becke, *J. Chem. Phys.* **1993**, *98*, 5648.
[33] C. Lee, W. Yang, R. G. Parr, *Phys. Rev. B* **1988**, *37*, 785.
[34] a) A. Schäfer, C. Huber, R. Ahlrichs, *J. Chem. Phys.* **1994**, *100*, 5829; b) F. Weigend, R. Ahlrichs, *Phys. Chem. Chem. Phys.* **2005**, *7*, 3297.
[35] M. Sierka, A. Hogekamp, R. Ahlrichs, *J. Chem. Phys.* **2003**, *118*, 9136.
[36] F. Weigend, *Phys. Chem. Chem. Phys.* **2006**, *8*, 1057.
[37] See Supporting Information for further computational details.

